Transactions of the 15th International Conference on
Structural Mechanics in Reactor Technology (SMiRT-15)
Seoul, Korea, August 15-20, 1999

Reactor Pressure Vessel Head Loaded by a Corium Slug Results of Model Experiments BERDA I

R. Krieg, B. Göller, G. Hailfinger, G. Messemer and G. Vorberg

Forschungszentrum Karlsruhe GmbH, Institut für Reaktorsicherheit, Germany

ABSTRACT

The load carrying capacity of the pressure vessel head to withstand an in-vessel steam explosion is investigated. First, as a key problem, the impact of molten core material against the vessel head is studied by model experiments scaled down 1:10. Structural details are carefully considered. The results are converted to reactor dimensions using similarity theory. This approach was checked by simplified liquid-structure impact experiments in different scale. Second, the upward acceleration of molten core is studied by computational models. As results the mechanical energies which the vessel head can withstand are presented.

1. INVESTIGATION STRATEGY

During a postulated in-vessel steam explosion molten core material may be accelerated as a liquid slug against the upper vessel head. If the head would fail, fragments of it could be hurled against the containment and endanger its integrity [1, 2]. Therefore, it is required that the liquid slug impact must not cause failure neither of the vessel head nor of the bolts connecting the head to the vessel flange.

In a first step – called BERDA I – the kinetic slug energy which can be carried by the vessel head and the bolts is determined. It is called the admissible kinetic slug energy E_{slug}. Assessments of the impact process revealed two facts which are expected to mitigate the loading and therefore to increase the admissible kinetic slug energy considerably [3]: The liquid character of the slug and the presence of upper internal structures underneath the vessel head. Due to these facts, the impact duration will be increased and thus for a given slug momentum the impact force is expected to decrease. Therefore, in our investigations, the slug is modeled as a liquid and the upper internal structures are considered.

In a second step - called BERDA II - the mechanical energy is determined, which must be fed into the upward acceleration of the core support plate, such that the admissible kinetic slug energy can be reached. It is called the admissible mechanical energy input E_{plate}. Here it is important to consider that the molten core material which is assumed to become the liquid slug is located on top of the core support plate. Thus, only a fraction of the mechanical energy input will be transferred into kinetic energy of the liquid slug.

Now, if the admissible mechanical energy input E_{plate} is higher than the mechanical energy release from the steam explosion, investigated elsewhere, then the above requirement is fulfilled: The vessel head and its bolts will not fail due to a steam explosion and the containment integrity will not be endangered.

2. DESCRIPTION OF THE MODEL EXPERIMENTS BERDA I

Since reliable computational methods for the slug impact problem are not available yet, the model experiments BERDA I are aimed to simulate the reactor scenario as close as possible, such that the results may be directly transferred to reactor conditions. Therefore, the vessel head and its bolts are represented by models made of the original materials. In most of the tests also models of the upper internal structures are included; in some cases they were made of the original material, in other cases, they were made of red brass in order to simulate the reduced material strength and ductility under accident conditions. All the models are precisely scaled down by 1:10. The molten core is simulated by liquid metal with about the same density but with a much lower melting temperature. So the test can be carried out close to room temperature. The liquid metal is contained in a crucible and accelerated against the model of the head using a pneumatic drive mechanism as shown in Fig. 1. Prior to the liquid slug impact the crucible is decelerated by a crash cylinder, thus the crucible does not participate in the impact process. To carry the dynamic loads, the whole facility is mounted on a heavy base plate of 38000 kg which is supported by springs.

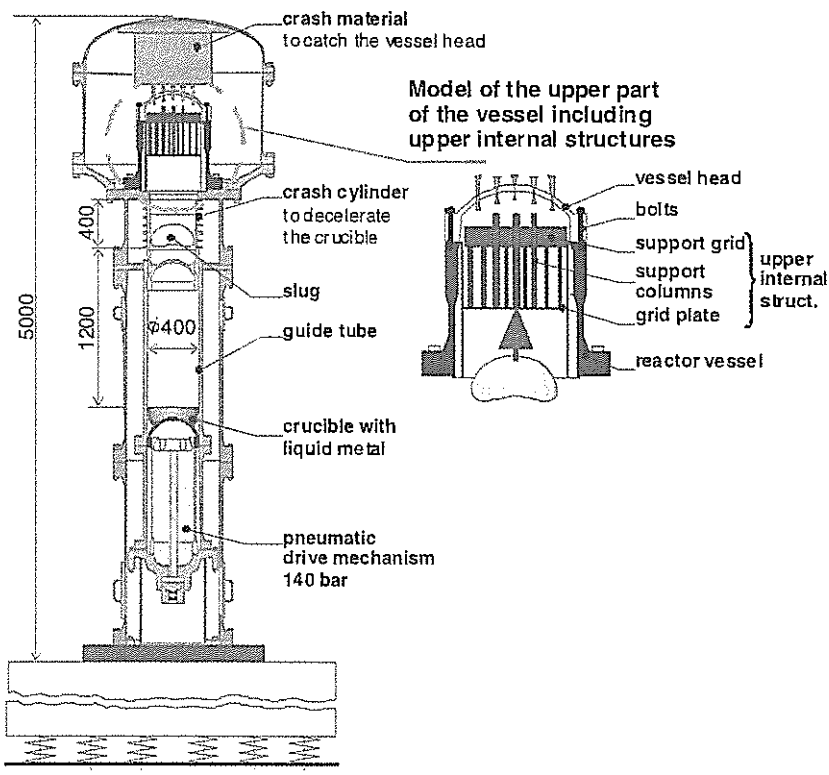

Fig. 1: Facility for the model experiments BERDA I

The liquid slug velocity is measured by photoelectric beams located at different positions along the slug path. The impact force is measured by strain gauges mounted at the bolts connecting the vessel head to the vessel flange. During the test the head deformation is also measured by strain gauges and afterwards by a three-coordinate measuring machine.

3. RESULTS OF THE MODEL EXPERIMENTS BERDA I

3.1 Impact of Slugs Consisting of Lead Spheres, Upper Internal Structures Neglected, Test 01 and 02

In the first and second test lead spheres of 10 mm diameter were filled into the crucible and accelerated against the head. The total mass of the spheres was 65 kg, the measured impact velocities were 78 m/s and 101 m/s, respectively. For simplicity, there was only one central hole of 12 mm diameter in the heads. The maximum impact force linearly converted to a slug mass of 80 kg and the permanent head displacements are shown in Fig. 2. In addition, for test 02 the force history is shown in Fig. 3. In both cases the time integration yielding the momentum transferred to the head approaches the initial momentum given by the product of slug mass and slug velocity. This is in line with the principle of momentum conservation, if one considers, that for the impact of lead spheres significant rebound effects do not occur. Here, one should refer to Fig. 4 showing strong plastic deformations of the spheres after the impact. Thus, we have additional evidence that the measurements are correct.

3.2 Impact of a Solid Slug, Upper Internal Structures Neglected, Test 03

For comparison in the third test a steel projectile with a spherical surface was hurled against the head; radius of the spherical surface 160 mm; radius of the inner surface of the head 278 mm. The mass of the projectile was only 26 kg, the measured impact velocity was 101 m/s. Again, there was only one central hole of 12 mm diameter in the head. The maximum impact force linearly converted to a slug mass of 80 kg is shown in Fig. 2. Consider that for the solid slug the maximum impact force is much higher than for test 02 with lead spheres, although the velocity was the same. Comparison of the momentum transferred during the first force peak with the initial momentum led to a rebound factor of 1.4.

3.3 Impact of Liquid Metal Slugs, Upper Internal Structures Neglected, Test 04 to 07 and 09

In order to simulate worst case conditions, rather compact slugs are desired. Therefore, the liquid metal was contained in a second, very thin-walled crucible, which was carried in the stronger crucible mentioned above. The second crucible was not decelerated by the crash tube but it moved on together with the liquid metal till the impact occurred. Thus, the slug mass consisted of the liquid metal of 80 kg plus that of the second crucible and the heater of 2.4 kg.

In test 04 the strong crucible failed during the deceleration by the crash tube. Thus, the impact mass was additionally increased by a crucible fragment of about 2.6 kg. Furthermore, the determination of the impact velocity was very difficult and ambiguous; it was assumed to be 118 m/s. The force history consists of several moderate peaks. The maximum force linearly converted to a slug mass of 80 kg is shown in Fig. 2. We assume that this result was largely influenced by the failed crucible which probably led to enhanced slug dispersion.

In test 05 to 07 and 09 the crucible remained intact. The impact velocities reached 110 m/s, 107 m/s, and two times 61 m/s, respectively. For these tests, heads were used with a pattern of control rod holes similar to that of German PWR of Convoy type; diameter of the central hole 12 mm, of the other holes 10 mm. The maximum impact forces linearly converted to a slug mass of 80 kg and the permanent head displacements are shown in Fig. 2. The deviations between test 07 and 09 are discussed later. As an example, for test 05 the force history is shown in Fig. 5. Now, the force histories contain only one major peak. The maxima are much higher, but the impact durations are shorter than obtained for test 04. The rebound factors were between 1.12 and 1.18. In order to give an impression of the head deformations, for test 05 the head before and after the impact is shown in Fig. 6. In

comparison with test 01 and 02, where slugs of lead spheres were used, the impact forces are slightly higher; the impact durations are about the same. However, in comparison with test 03 with the solid slug the impact forces are much lower.

In test 06 an additional hole was drilled close to the central hole, where the highest strain occur. Consequently, in this local area a through wall crack developed, as shown in Fig. 7. Before the tests the holes were closed by plugs with threads similar to German PWR. During the slug impact of test 05 and 06 many plugs were expelled reaching velocities up to about 80 m/s.

All the results up to test 07 were also presented and discussed in [4].

3.4 Impact of Liquid Metal Slugs, Upper Internal Structures of Original Steel Considered, Test 08, 10, 12 and 15

The details of the liquid metal slugs were the same as before. The impact velocities were 106 m/s, 121 m/s, 131 m/s and 129 m/s, respectively. The upper internal structures before the impact are shown in Fig. 8. Also the control rod drives inside the tubes were roughly simulated. Now the maximum impact forces linearly converted to a slug mass of 80 kg are shown in Fig. 9. As an example, for test 12 the force history is shown in Fig. 10. The impact forces are much lower and the impact durations are much longer than in the tests without upper internal structures. The rebound factors were between 1.08 and 1.14. Permanent head deformations did not occur, although in most of the tests the impact velocities were higher than before. However, the upper internal structures were heavily deformed, see Fig. 11.

3.5 Impact of Liquid Metal Slugs, Upper Internal Structures of Red Brass Considered, Test 11, 13 and 16

The details of the liquid metal slugs were the same as before. The impact velocities were 130 m/s, 128 m/s and about 160 m/s, respectively. However, in test 16 the crucible failed, and therefore, the determination of the velocity of 160 m/s is questionable. Also the geometry of the upper internal structures was the same as before, however, now the material was red brass and for test 16 the material of the control rod guide tubes was lead. The force histories were similar as before, except test 13, where the maximum force occurred as a peak with a very short duration of only about 0.4 ms. Therefore, it is called the peak maximum. The remaining force history reached a smaller maximum called bulk maximum. The maximum impact forces, linearly converted to a slug mass of 80 kg are shown in Fig. 9. For test 11 and 13 the force histories are shown in Fig. 12. It turns out that the weaker and more brittle upper internal structures made of red brass have no significant influence on the loads, except the narrow peak discussed above. The rebound factors were 1.26 and 1.28, which is noticeable higher than before. For test 11 and 13 permanent head deformations did not occur. The upper internal structures broke into many pieces. Thus the resulting fragments are very different from the large deformations observed for structures made of steel. For test 11 the fragments are shown in Fig. 13.

3.6 Impact of a Liquid Metal Slug, only an Upper Support Grid of Steel Considered, Test 14

The liquid metal slug was similar to those before. The impact velocity was 108 m/s. However, the thickness of the upper support grid had been reduced to 75 % of its nominal value. The maximum force linearly converted as before, and the very small permanent head displacement are shown in Fig. 9. One can see that the maximum force is about twice the corresponding value obtained with the complete upper internal structures, but it is still considerably lower than the values without any upper internal structures.

3.7 Impact of Liquid Metal Slugs, only Upper Support Grids of Red Brass Considered, Test 17, 19 and 20

Again, the liquid metal slugs were similar as before. The impact velocities were 126 m/s, 106 m/s and 103 m/s, respectively. The maximum forces occurred as peaks like observed for test 13. Both, the peak and the bulk maxima linearly converted as before and the permanent head displacements are shown in Fig. 9. As an example, for test 19 the impact force history is shown in Fig. 14. Comparison of test 19 and 20 with test 14 reveals, that the weaker and more brittle support grid made of red brass can be assumed to have caused the relatively high peak maxima, probably by the impact of upper grid fragments. However, the weaker and more brittle support grid has increased the permanent head deformations only slightly.

One can confirm that the peak maxima have not the same effect as the other maximum forces: For test 19 and 20 the peak forces reach about the same values as for test 05 and 06 the maximum forces; but for test 19 and 20 the permanent head displacements are much lower than for test 05 and 06.

4. INTERPRETATION OF THE MODEL EXPERIMENTS BERDA I

4.1 Application of Computational Models

Analysis of the liquid structure impact process was carried out with the code PLEXUS [5]. The liquid was modeled by a large number of particles, the vessel head by finite elements. Using about 20 000 particles the test 07 could be fairly simulated. However, despite of this high number of elements requiring large computational effort convergence was not obtained. So the reliability of the predictions is questionable. Furthermore, modeling of the upper internal structures is still an unsolved problem.

The deviation between test 07 and 09 was studied with the finite element code ABAQUS. It turned out that the somewhat higher impact force and the smaller head displacement of test 09 may be caused by increasing the impact area at the head. This might be due to slightly varying slug acceleration conditions leading to increased radial slug dispersion. It is interesting to note, that with upper internal structures severe deviations between similar tests have not been observed.

For better understanding of the various impact phenomena the special code SimSIC was developed [6]. It must be mentioned, however, that this code needs some input obtained from experiments. In Fig. 2 the curve describing the maximum impact force as a function of the impact velocity could be explained with SimSIC. The change of the inclination of this curve at a velocity of about 60 m/s is due to the onset of plastic head deformation.

4.2 Transfer of the Results to the Reactor Scale

Conversion of the test results to the reactor scale is accomplished using similarity theory. The length scale λ_ℓ is given by the ratio between the reactor dimensions and the corresponding model dimensions. For BERDA I it is $\lambda_\ell = 10$. The stress scale λ_σ is given by the ratio between the stresses in the stress-strain diagrams for the reactor and the corresponding stresses in the diagrams for the model. Considering that the reactor vessel head has a temperature of 300 – 400 °C, while the model head is at room temperature, we found $\lambda_\sigma = 0.87$.

Now using the conventional basic equations including the equilibrium conditions, the constitutive equations for time-independent elastic-plastic material behavior, etc., the scales for other quantities can be derived:

$$\text{time scale} = \lambda_\ell/\sqrt{\lambda_\sigma} = 10.7; \qquad \text{velocity scale} = \sqrt{\lambda_\sigma} = 0.93;$$

$$\text{force scale} = \lambda_\ell^2 \lambda_\sigma = 87; \qquad \text{energy scale} = \lambda_\ell^3 \lambda_\sigma = 870.$$

The strains are the same for both the reactor and the model.

Since the basic equations allow only an approximative description of the problem, the scaling rules have also an approximative character. To check the deviations, the similarity experiments FLIPPER had been carried out, where a simple liquid-structure impact process was investigated in three different scales [6]. For the ferritic steel of the vessel head a moderate scale influence was found which could be explained by the known strain rate effect on the stress-strain diagram. This effect was considered when defining the above values. However, for austenitic steel, where the upper internal structures are made from, a strong deviation was found indicating that the conventional constitutive equations are not adequate here. Fortunately, this is of minor importance, since the influence of the material properties of the upper internal structures on the head response had turned out to be rather low.

The scaling rules apply also to non-linear processes and plastic deformations. However, material damage and fracture could not be taken into account, as adequate theoretical models do not exist. That means, failure strains obtained in the model tests cannot be expected to be possible in the reactor components. Therefore, only those results of model experiments BERDA I were converted to the reactor scale, where the plastic head deformations are so small that fracture can be ruled out even for reactor dimensions.

4.3 Determination of the Admissible Slug Energy E_{slug} for the Reactor Scale

Following the above rules, the admissible slug energy can be determined for three cases:

Case **A**, all upper internal structures are molten. Fig. 2 (test 07 and 09) yields $\mathbf{E_{slug} = 0.1\ GJ.}$

Case **B**, only the support grid is available. Fig. 9 (test 14, 19 and 20) yields $\mathbf{E_{slug} = 0.4\ GJ.}$

Case C, all upper internal structures. Fig. 9 (extrapol. test 08, 10, etc.) yields $\mathbf{E_{slug} = 0.8\ GJ.}$

5. ASSESSMENT OF THE MODEL EXPERIMENTS BERDA II

The model experiments BERDA II are aimed to simulate the upward acceleration of the core support plate carrying the molten core material. Of special interest is, how this molten core material will form a liquid slug. Currently, the test facility is going to be erected. Since test results are not available yet, assessments by computational models are presented.

The problem is sketched in Fig. 15. The kinetic slug energy E_{slug} of the molten core material hurled upwards is

$$E_{slug} = \int F_0 \, ds_0 = m_0 \int a_0 ds_0$$

with the acceleration force F_0, the mean acceleration path s_0, the molten core mass m_0 and the mean acceleration a_0.

During acceleration, the geometrical form of the core melt may change. In particular, radial acceleration components may occur leading to radial liquid dispersion. Thus the energy input E_0 into the molten core mass may be higher than E_{slug} .

$$E_0 = \int F_0 \, ds_1 = m_0 \int a_0 ds_1$$

Due to equilibrium reasons, the applied force must be equal to the acceleration force F_0. During radial liquid dispersion, however, the acceleration path s_1 and the acceleration a_1 at the surface of the molten core mass prescribed by the core support plate may be larger than the mean acceleration path s_0 and the mean acceleration a_0 of this mass.

The kinetic energy of the core support plate is

$$E_1 = \int F_1 \, ds_1 = m_1 \int a_1 ds_1$$

with the acceleration force F_1 and the plate mass m_1.

Neglecting the compression of the core barrel, the mechanical energy input E_{plate} at the core support plate is $E_{plate} = E_0 + E_1$.

In case of an unrestricted radial core melt dispersion, the acceleration ratio χ causing approximately the same path ratio $\chi = a_0/a_1 \approx s_0/s_1$

above all depends on the core melt geometry and can be calculated by an available code.

Then, using the above equations one obtains

$$E_{plate} = E_{slug}\left[1/\chi + 1/\chi^2\,(m_1/m_0)\right].$$

It should be mentioned that the deceleration of the core support plate by compression of the core barrel does not contribute to the maximum impact of the vessel head and its bolts. The cross section of the core barrel limits the force transferred to the bolts. Furthermore, this force occurs prior to the liquid slug impact against the vessel head.

Four cases **a, b, c, d** as indicated in the left hand column of Fig. 16 were studied. For case **a** no radial melt dispersion is assumed, i.e. $\chi = 1.0$. For the other cases radial melt dispersion possibly causing core barrel expansion is allowed and the acceleration ratios $\chi < 1.0$ were calculated. The resulting admissible mechanical energy input E_{plate} for the three different slug impact cases at the vessel head **A, B, C** are listed in Fig. 16.

5. FINAL REMARKS AND CONCLUSIONS

The load carrying capacity of the reactor vessel head described in terms of admissible kinetic slug energies has been obtained under quite pessimistic conditions: The liquid slug representing the molten core material was assumed to be rather compact. In addition, only minor plastic head deformation were allowed, since reliable knowledge about the failure strain of large structural components is not available yet. However, there are indications that the failure strains are not significantly smaller than the high values reached in test 05 and 06. If this can be confirmed by investigations which have been started recently, the admissible kinetic slug energies can be increased.

The admissible energy inputs at the core support plate have been assessed, too. But these values need confirmation by the model experiments BERDA II. In addition, case **A** is expected to be irrelevant, since melting of all the upper internal structures is very unlikely.

If necessary, also other mechanical energy sinks such as flow processes in the lower head region and deformation of the lower head of the reactor pressure vessel may be considered. Thus, there is a good chance that the admissibly value will be higher than the mechanical energy release from the steam explosion, and as a consequence that the vessel head and its bolts will not fail and the containment integrity will not be endangered.

ACKNOWLEDGEMENT

This work was partly executed within the research project RPVSA co-financed by the European Commission under the Nuclear Fission Safety program 1994 – 1998.

REFERENCES

[1] G. Keßler, J. Eibl, "Severe Accident Containment Loads and Possible Design Concepts of Future Large Pressurized Water Reactors", *Nucl. Technol.*, 111, 358 (1995)

[2] G.E. Lucas, W.H. Amarasooriya, T.G. Theofanous, "An Assessment of Steam-Explosion-Induced Containment Failure, Part IV", *Nucl. Sci. Eng. 97*, 316 (1987)

[3] R. Krieg, T. Malmberg, G. Messemer, T. Stach, E. Stratmanns, "Slug Impact Loading on the Vessel Head during a Postulated In-vessel Steam Explosion in Pressurized Water Reactors", *Nucl. Technol. 111*, 369 (1995)

[4] R. Krieg, T. Malmberg, G. Messemer, G. Hoffmann, T. Stach, E. Stratmanns, "Model Experiments BERDA Describing the Impact of Molten Core Material against a PWR Vessel Head", *Int. Conf. on Advanced Reactor Safety ARS'97*, Orlando, USA (June 97)

[5] H. Bung, P. Galon, M. Lepareux, A. Combescure, "PLEXUS, A new Method for the Treatment of Impact and Penetration Problems", *SMIRT 12*, Stuttgart 1993, paper B02/1

[6] A. Hirt, "Rechenmodell zum Aufprall von Kernschmelze auf die oberen Einbauten und den Deckel eines Reaktordruckbehälters", PhD thesis, Universität Karlsruhe (1997)

[7] T. Stach, T. Malmberg, R. Krieg, "Scaled Experiments for a Simple Deformable Structure under Liquid Slug Impact", *SMIRT 14, Lyon 1997*, paper P02/1

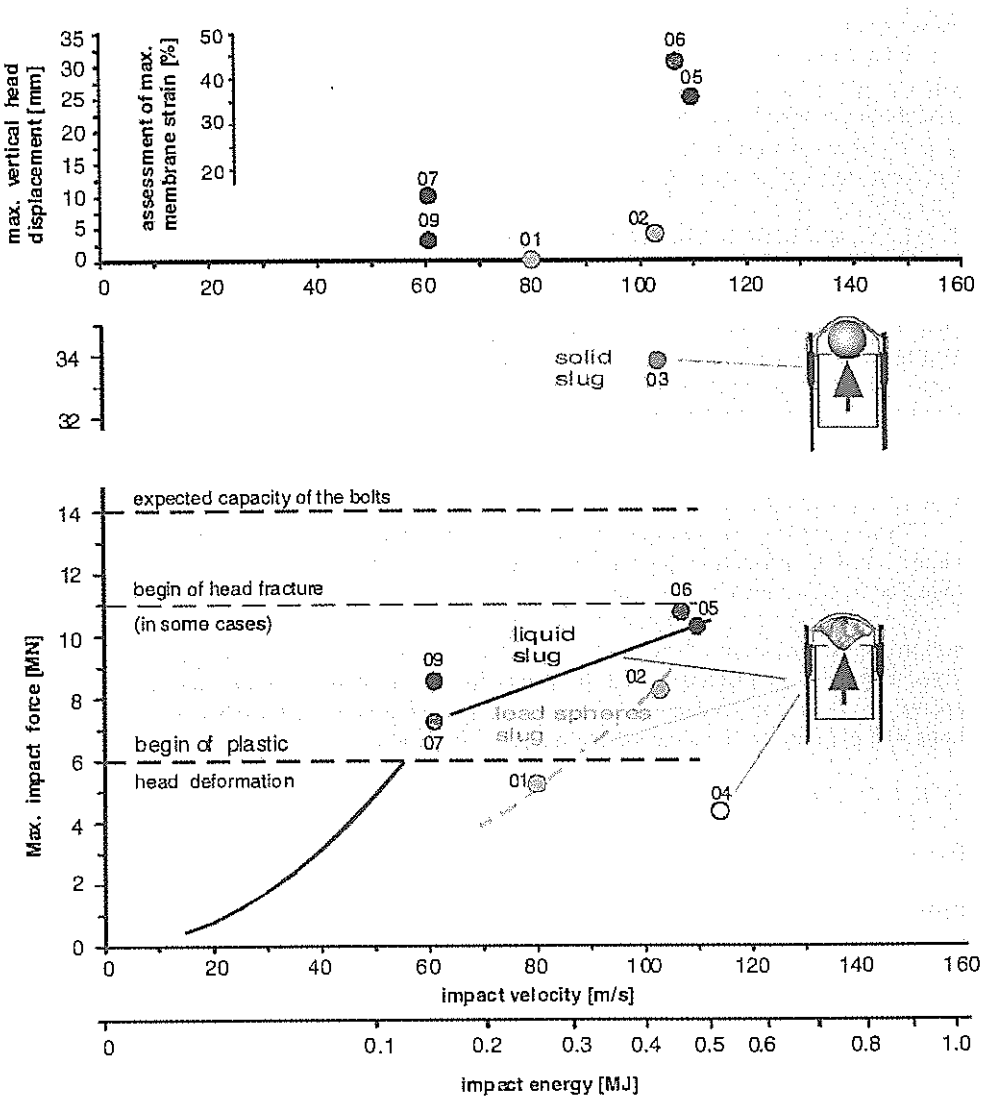

Fig. 2: Results for tests without upper internal structures

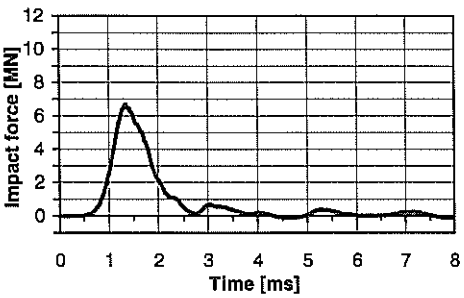

Fig. 3: Test02, lead spheres, 65 kg, 101 m/s, upper internal structures neglected.

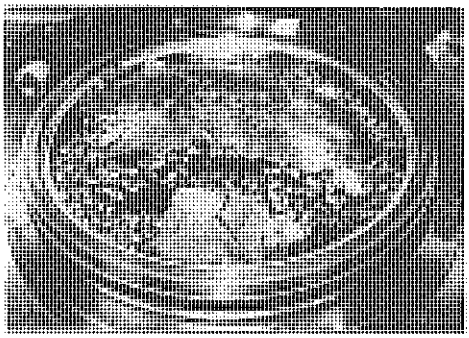

Fig. 4: Test02, plastic deformations of the lead spheres after the impact.

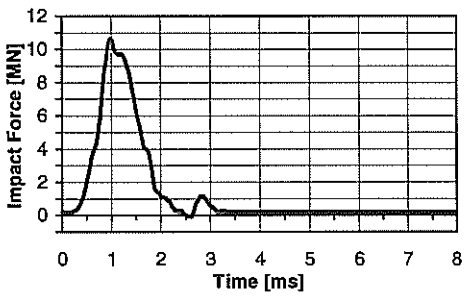

Fig. 5: Test05, liquid metal, 80 kg, 110 m/s, upper internal structures neglected.

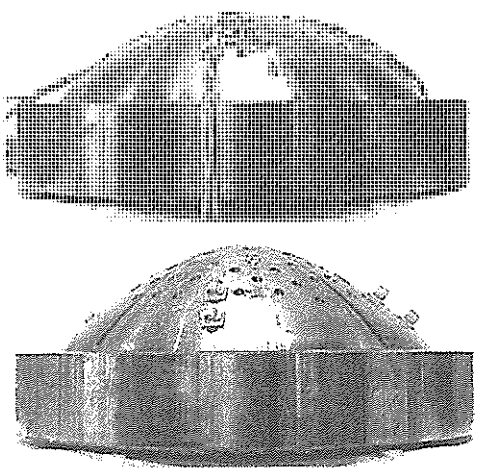

Fig. 6: Test05, shape of the head before and after the impact

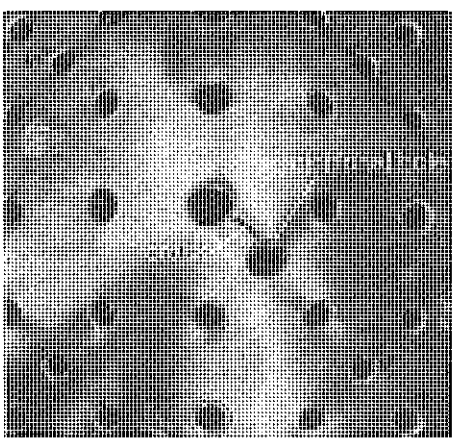

Fig. 7: Test06.
During the head deformation a crack developed.
In addition, the holes in the head were increased and many plugs which had closed the holes were expelled.

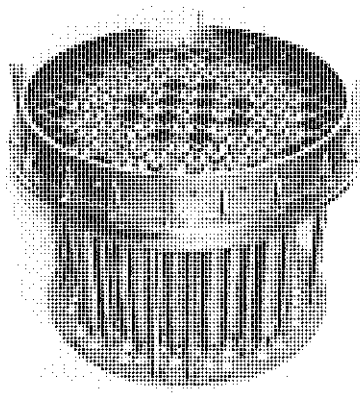

Fig. 8: Model of the upper internal structures prior to the slug impact

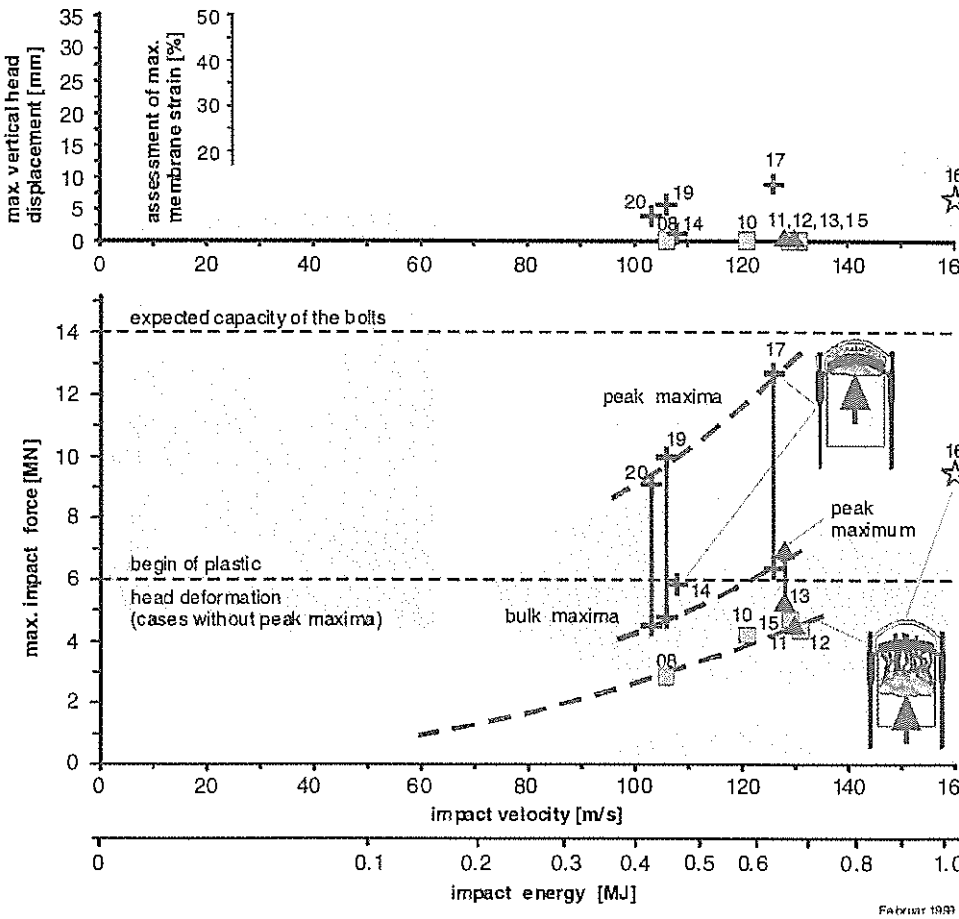

Fig. 9: Results for liquid slug impact tests with upper internal structures

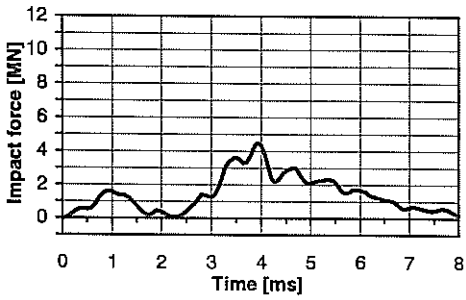

Fig. 10: Test12, liquid slug, 80 kg, 131 m/s, upper internal structures of steel.

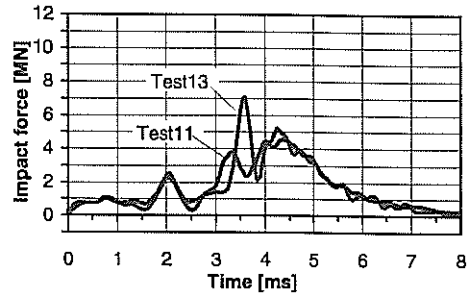

Fig. 12: Test11 and 13, liquid slug, 80 kg, 130 m/s and 128 m/s, upper internal structures of brass.

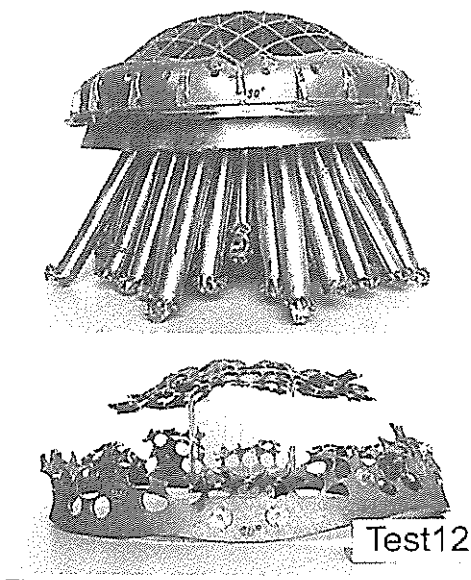

Fig. 11: Test12, upper internal structures of steel after the slug impact.

Fig. 13: Test11, upper internal structures of brass after the slug impact.

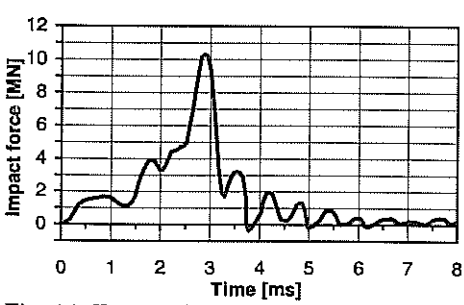

Fig. 14: Test19, liquid slug, 80 kg, 106 m/s, only upper support grid considered.

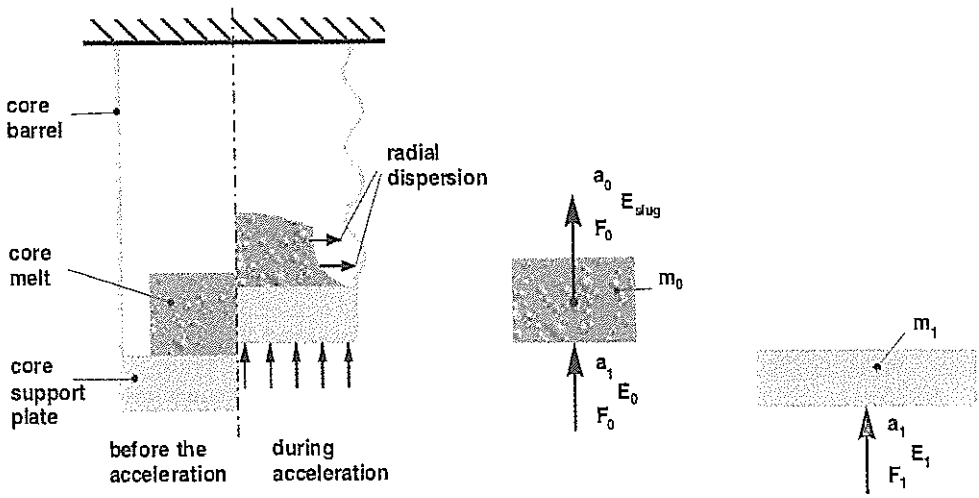

Fig. 15: Computational model to accelerate the core support plate and the molten core

	upper line: mass of the heavy reflector not considered lower line: half of the mass of the heavy reflector added to the mass of the support plate	A Upper int. struct. molten E_{slug} = 0,1 GJ	B Only upper grid available E_{slug} = 0,4 GJ	C Upper int. struct. available E_{slug} = 0,8 GJ
a	3,9 m Ø, concertina mode, χ = 1.0	E_{plate} = 0,15 GJ 0,20	Because of high E_{slug} concertina mode not expected	
b	3,9 m Ø, radial expansion, χ = 0.7	Because of small E_{slug} rad. expansion not expected	E_{plate} = 1,0 GJ 1,4	2,0 2,8
c	3,3 m Ø, χ = 0.5	0,4 0,6	1,6 2,4	3,2 4,8
d	conical, χ = 0.4	0,5 0,8	2,2 3,5	4,4 7,0

Fig. 16: Calculated admissible mechanical energy input E_{plate}